ANNALS of Clinical and Translational Neurology
Open Access
AMERICAN NEUROLOGICAL ASSOCIATION

RESEARCH ARTICLE

Brain lesion characteristics in Chinese multiple sclerosis patients: A 7-T MRI cohort study

Lei Su[1,2,#], Zhe Zhang[1,#], Chenyang Gao[1,2], Ai Guo[1], Mengting Zhang[1], Xiaoyu Shi[1], Xinyao Liu[1], Tian Song[1], Wangshu Xu[1], Huabing Wang[1], Joseph Kuchling[3,4], Jing Jing[1], De-Cai Tian[1], Yaou Liu[1], Yunyun Duan[1], Friedemann Paul[3,4] & Fu-Dong Shi[1,2]

[1]Departments of Neurology, Radiology, Tiantan Neuroimaging Center of Excellence, China National Clinical Research Center for Neurological Diseases, Beijing Tiantan Hospital, Capital Medical University, Beijing, China
[2]Department of Neurology, Tianjin Medical University General Hospital, Tianjin, China
[3]Experimental and Clinical Research Center, Max Delbrueck Center for Molecular Medicine and Charité-Universitätsmedizin Berlin, Humboldt Universität zu Berlin, Berlin Institute of Health, Berlin, Germany
[4]Department of Neurology, Charité-Universitätsmedizin Berlin, Berlin, Germany

Correspondence
Fu-Dong Shi, Beijing Tiantan Hospital, Capital Medical University, No.119 South 4th Ring West Road, Fengtai District, Beijing 100070, People's Republic of China. Tel: +86 010-59978545; Fax: +86 010-59975650.
E-mail: fshi@tmu.edu.cn

Received: 3 March 2024; Revised: 4 October 2024; Accepted: 29 October 2024

doi: 10.1002/acn3.52256

[#]Equal contribution.

Abstract

Objective: Prevalence, susceptibility genes, and clinical and radiological features may differ across different ethnic groups of multiple sclerosis (MS). We aim to characterize brain lesions in Chinese patients with MS by use of 7-T MRI. **Methods**: MS participants were enrolled from the ongoing China National Registry of Neuro-Inflammatory Diseases (CNRID) cohort. 7-T MRI of the brain was performed. Each lesion was evaluated according to a standardized procedure. Central vein sign (CVS) and paramagnetic rim lesions were identified. The characteristics of lesions at patient-level and at lesion-level from previous 7-T MRI literature were also summarized. **Results**: We included 120 MS patients. Their mean (SD) age was 34.6 (9.4) years. The female-to-male ratio was 1.7:1 and mean disease duration of patients with MS was 5.5 ± 6.1 years. The median EDSS score was 2 (range, 0–8). A total of 8502 lesions were identified with a median lesion count of 45 (IQR, 18–90) (range, 2–370). The median (IQR) percentage for these special locations were as follows: cortical lesions (CLs) 2.7% (0%–5.7%), juxtacortical lesions 16.2% (7.8%–25.7%), periventricular lesions 30.2% (17.2%–38.7%), and infratentorial lesions 5.8% (0.4%–11.9%). CLs occurred in 70 (58%) patients, accounting for only 443 (5%) of the total lesions. Out of the 443 CLs, 309 (69.8%) were leukocortical lesions. CVS appeared in 5392 (63%) lesions from 117 (98%) patients. 1792 (21%) lesions and 104 (87%) patients exhibited a paramagnetic rim. **Interpretation**: Our study elaborated on the lesion features of Chinese patients with MS by use of 7-T MRI. Lesion burden is heavy in Chinese patients with MS. The median lesion count and proportion of PRL are high. The reported heavy lesion burden calls for ramping up regional and global efforts to care for MS patients. The management and research of Chinese population with MS needs to be further strengthened.

Introduction

Multiple sclerosis (MS) is an immune-mediated demyelinating disease of the central nervous system, and it is a leading cause of disability among young adults worldwide.[1] Gene–environment interactions drive susceptibility risk and structural brain alterations in MS. China is a vast eastern country characterized by considerable regional and genetic differences from Western population. However, it remains unclear whether the brain lesion characteristics in Chinese patients with MS are of a distinct nature.

Genetic inheritance is associated with MS susceptibility and phenotype. In cohorts of European descent, there are

distinctive associations between polygenic inheritance and risk of tissue damage and imaging outcomes. For instance, genetic predisposition is associated with changes in brain structure in MS patients, characterized by thalamic atrophy.[2] African ancestry is also a risk factor for a more rapidly disabling disease course.[3] Compared to Caucasian Americans with MS, African Americans with MS demonstrate more pronounced brain tissue damage, such as gray matter atrophy and increased lesion burden.[4] Furthermore, there are significant differences in the incidence, peak age of onset,[5,6] susceptibility genes,[7,8] and effectiveness of DMT[9] in Chinese MS patients compared to Western populations, but there is a paucity of studies examining the brain substructure alterations in Chinese MS patients.

Brain lesions in MS are well-characterized and, with advances in technology, new imaging markers are becoming increasingly recognized. Cortical lesions (CLs) contribute to physical and cognitive disability in MS.[10] The central vein sign (CVS)[11] is emerging as an imaging marker for the diagnosis of MS, which has shown the ability to accurately differentiate MS from other white matter diseases (MS mimics).[12] Meanwhile, paramagnetic rim lesions (PRL) are specific to MS,[13] and are considered to be chronic active lesions, a novel imaging feature predictive of disease progression. CL and PRL can also be used for the differential diagnosis of MS.[14] Due to its increased signal-to-noise ratio, spatial resolution and susceptibility effects,[15] 7-T MRI has potential advantages compared to lower field strengths, in the identification of MS lesions, CVS, and PRL judgment.

It is urgent and imperative to characterize the imaging features of the Chinese MS population in a large 7-T MRI cohort. With this background, we aim to determine the characteristics of brain lesion distribution, the proportion of CVS and PRL and their relationship with disease duration and MS-associated disability using 7-T MRI within the China National Registry of Neuro-Inflammatory Diseases cohort (CNRID).

Materials and Methods

Participants

We analyzed the data from an ongoing CNRID cohort to investigate the clinical status and imaging characteristics of Chinese patients with inflammatory demyelinating disease (IDD). Details about this cohort are available in ClinicalTrials.gov (Identifier: NCT05154370). In total, 120 patients with MS were enrolled from CNRID between December 2021 and December 2022. Inclusion criteria were the following: age of 18 years or older, diagnosis of MS according to the revised 2017 McDonald criteria,[1] and no clinical relapse within the preceding 3 months.

MRI data acquisition

All participants underwent 7T MR imaging (MAGNETOM Terra, Siemens Healthcare, Erlangen, Germany) using a 32-channel Rx/8Tx head-coil (Nova Medical, Wilmington, Massachusetts, USA) at Beijing Tiantan Hospital. The scanning procedure consisted of 3D magnetization prepared rapid acquisition gradient echoes (T1-MPRAGE) sequence to cover the whole brain (TR = 2200 ms, TE = 3.0 ms, TI = 1050 ms, matrix = 320 × 320, isotropic resolution of 0.7 × 0.7 × 0.7 mm^3, total acquisition time = 6 min 29 s), fluid-attenuated inversion recovery (FLAIR) (TR = 6600 ms, TE = 95 ms, TI = 2200 ms, matrix = 336 × 235, in-plane resolution of 0.3 × 0.3 mm^2, slice thickness of 2 mm, and total acquisition time = 5 min 18 s), susceptibility weighted imaging (SWI) (TR = 19 ms, TE = 12 ms, matrix = 640 × 640, in-plane resolution of 0.1 × 0.1 mm^2, slice thickness of 1.2 mm, and total acquisition time = 7 min 45 s), and multi-echo T2*-weighted spoiled gradient echo sequences (TR = 2500 ms, TE = 10, 20, 30 ms, matrix = 800 × 700, in-plane resolution of 0.1 × 0.1 mm^2, slice thickness of 1.2 mm, and total acquisition time = 9 min 34 s). FLuid And White matter Suppression (FLAWS) based on the magnetization prepared with two rapid gradient echoes (MP2RAGE) sequence (FLAWS-MP2RAGE) was adopted for better detecting lesions (TR = 5000 ms, TE = 1.44 ms, TI1/TI2 = 700/1700 ms, Matrix = 256 × 256, isotropic resolution of 0.75 × 0.75 × 0.75 mm^3, and total acquisition time = 8 min 52 s). The FLAWS-MP2RAGE sequence produces three sets of images including two inversion times (INV1 and INV2) and a corrected image (UNI) (Supplementary Section 1).

Image analysis

Lesions were analyzed and labeled in 3D Slicer (Version 4.6.2, https://www.slicer.org/). All MRI images were analyzed independently and blindly step by step according to a standardized procedure (Supplementary Section 2). After training, two experienced neuroradiologists (C. Gao and L. Su), who were blinded to the patients' clinical data, assessed independently, with a third neuroradiologist (Y. Duan) determining when inconsistencies were encountered.

T1-MPRAGE and T2-FLAIR were used to identify lesions. Hypointense T1 lesions were marked and segmented manually on T1-MPRAGE image, with simultaneous reference to the T2-FLAIR image. Combined with FLAWS, lesion location was identified. According to its anatomical location, each lesion was categorized as either cortical (lesion involved within the cerebral cortex), juxtacortical (adjacent to cortical gray matter or subcortical U-fibers), periventricular (immediately adjacent to the

ventricles), and infratentorial (lesion in the brainstem, cerebellar peduncles, or cerebellum). T2*WI and SWI (Siemens MR scanner is a left-handed system and paramagnetic substances show hyperintense signal on phase images; the phase positivity can be opposite to that on right-handed systems[16,17]) were used to identify CVS and PRL, respectively. In each individual, CVS was defined in accordance with the North American Imaging in MS Cooperative criteria,[18] and the number of PRL was determined on phase images.[19] Lesion size was calculated automatically based on the manually defined lesion mask and known imaging voxel size (Supplementary Section 2).

A quantitative probability analysis approach was used to document the distribution of brain lesions. MRI data were analyzed using the FMRIB Software Library of tools (University of Oxford, UK). The segmented lesions were then registered to the Montreal Neurological Institute (MNI) 1-mm standard space template using a nonlinear transformation method (FNIRT [FMRIB's nonlinear image registration tool]). The nonlinear transformation matrix was then applied to the respective lesion segmentation masks to transform them into the space of the standard template. After transformation, the lesion masks were thresholded at 50% and binarized again to avoid the volume increase caused by the trilinear interpolation. They were then summed and averaged for each subject group to create lesion probability maps.[20]

Clinical assessment

Clinical data were collected for all patients, including disease duration and Expanded Disability Status Scale (EDSS). According to the disease duration, participants were stratified into a short course group (no more than 3 year) and a long course group (more than 3 years). According to the neurologic disability assessed by the EDSS score, participants were stratified into a moderately/highly disabled group (EDSS score more than 3.0) and a low disabled group (EDSS score was 3.0 or less).

Literature review

To compare the MS lesions characteristics with those from previously reported 7-T MRI studies, a comprehensive literature review was conducted, which included the patient-level prevalence and the lesion-level prevalence of CL and positive CVS lesions and PRLs (patient-level prevalence was defined as the proportion of patients with CL or positive CVS lesions or PRL, while lesion-level prevalence was defined as the proportion of total lesions identified as CL or positive CVS lesions or PRL) from previous 7-T MRI studies (Supplementary Section 3).

Statistical analysis

All statistical analyses were performed using SPSS software (V.22; SPSS, Chicago, Illinois, USA). Normality was determined for continuous variables using the Shapiro–Wilk test. Continuous variables following a normal distribution were expressed as means ± standard deviation (SD); otherwise, they were presented as median (interquartile range; IQR). Categorical variables were reported as frequencies and percentages. The *t*-test and Mann–Whitney *U*-test were used to compare continuous variables between the two subgroups. The chi-squared test and Fisher's exact test were used to compare categorical variables between the two subgroups. Partial correlation was performed to investigate the relationship between the MRI indices and EDSS with covariate adjustment including age and disease duration. The count and volume of total lesions and lesions in specific location significantly correlated with disability as measured by the EDSS score. The intraclass correlation coefficient (ICC) (two-way, alpha model, absolute agreement type) was employed to calculate inter-rater variability. Statistical significance was defined as a two-sided p-value < 0.05.

Results

Baseline data for the patients with MS

Baseline characteristics for patients with MS are shown in Table 1. In total, 120 participants with MS (111 relapsing–remitting and 9 progressive) were recruited. The mean disease duration of patients with MS was 5.5 ± 6.1 years. The median EDSS score was 2 (range, 0–8). 59 (49%) patients received disease-modifying therapy (DMT) at the time of MRI. Compared with RRMS, PMS patients were older (42.1 ± 11.5 vs. 33.9 ± 9.0, $p = 0.038$), had a longer disease duration (13.0 ± 4.1 vs. 4.9 ± 5.9, $p < 0.001$), and had a more severe EDSS score (6.0 [range, 2–6.5] vs. 2.0 [range, 0–8.0], $p < 0.001$) (Table 1).

Brain lesion characteristics in Chinese MS patients

A total of 8502 lesions were detected, and total lesion volume was 988.4 cm^3. Regarding the MS specific location, the proportion of CL 5% (443/8502) was the least frequent lesion type observed, followed by infratentorial lesions 8% (663/8502), periventricular lesions 23% (1932/8502), and juxtacortical lesions 26% (2220/8502). Of the 443 CLs, 309 (69.8%) were leukocortical, while the remaining 134 (30.2%) were either subpial or intracortical. The median (IQR) percentage for these special

Table 1. Demographic characteristics in MS cohort.

Characteristic	MS (n = 120)	RRMS (n = 111)	PMS (n = 9)	Statistical analysis
Age, years	34.6 (9.4)	33.9 (9.0)	42.1 (11.5)	$p = 0.038$
Female sex, No. (%)	76 (63)	70 (63)	6 (67)	$p = 1.000$
Disease duration, years	5.5 (6.1)	4.9 (5.9)	13.0 (4.1)	$p < 0.001$
EDSS score, median (range)	2 (0 to 8.0)	2 (0 to 8.0)	6.0 (2 to 6.5)	$p < 0.001$
Disease-modifying treatment, No. (%)	59 (49)	56 (50)	3 (33)	$p = 0.521$
Teriflunomide, No. (%)	29 (49)	28 (50)	1 (33)	$p = 1.000$
Interferon β-1b, No. (%)	2 (3)	2 (4)	0	$p = 1.000$
Fingolimod, No. (%)	3 (5)	3 (5)	0	$p = 1.000$
Siponimod, No. (%)	20 (34)	18 (32)	2 (67)	$p = 0.545$
Dimethyl fumarate, No. (%)	2 (3)	2 (4)	0	$p = 1.000$
Ofatumumab, No. (%)	3 (5)	3 (5)	0	$p = 1.000$

locations was as follows: CLs was 2.7% (0%–5.7%), infratentorial lesions was 5.8% (0.4%–11.9%), juxtacortical lesions was 16.2% (7.8%–25.7%), and periventricular lesions was 30.2% (17.2%–38.7%). At patient-level, we found CL in 70 (58%) participants, infratentorial lesions in 90 (75%) participants, juxtacortical lesions in 108 (90%) participants, and periventricular lesions in 117 (98%) participants (Figs. 1 and 2).

A total of 5392 (63%) lesions (median, 71%; range, 0%–100%) had CVS, and 1793 (21%) (median, 16%; range, 0%–67%) lesions exhibited a paramagnetic rim. CVS appeared in 43% of CLs (median, 50%; range, 0%–100%), 53% of juxtacortical lesions (median, 60%; range, 0%–100%), 55% of periventricular lesions (median, 60%; range, 0%–100%), and 68% of infratentorial lesions (median, 75%; range, 0%–100%). A paramagnetic rim was observed in 6% of infratentorial lesions (median, 0%; range, 0%–100%), 14% of CLs (median, 0%; range, 0%–100%), 20% of juxtacortical lesions (median, 9%; range, 0%–100%), and 22% of periventricular lesions (median, 17%; range, 0%–100%). For patient-level prevalence, CVS positive lesions were present in 118 (98%) patients and PRLs in 104 (87%) patients.

CL volume was higher in PMS (median, 101 mm^3; IQR, 54–821 mm^3) compared to RRMS (median, 19 mm^3; range, 0–192 mm^3) ($p = 0.03$). There was an increasing trend in the number of CL in PMS compared with RRMS, but there was no statistical difference. There was also no difference in the volume and count of lesions in the remaining specific location between RRMS and PMS. Cortical, juxtacortical, periventricular and total lesion volume were higher in patients with long disease duration (>3 years) compared to patients with short disease duration (≤3 years) ($p = 0.029$; $p = 0.020$; $p < 0.001$; $p = 0.001$, respectively). However, there was no significant difference in the lesion count between long and short disease duration group. Cortical, juxtacortical, periventricular, infratentorial, and total lesion count was higher in the moderately/highly disabled patient group (EDSS score > 3.0) compared with the low disabled group (EDSS score ≤ 3.0) ($p = 0.0036$; $p = 0.0012$; $p = 0.0026$; $p = 0.0015$; $p = 0.0012$, respectively). The volume of cortical, juxtacortical, periventricular, infratentorial, and total lesions was also higher in moderately/highly disabled group (EDSS score > 3.0) compared with low disabled group (EDSS score ≤ 3.0) ($p = 0.0018$; $p = 0.0053$; $p = 0.0120$; $p = 0.0012$; $p = 0.0023$, respectively) (Table 2). The count and volume of total lesions and lesions in specific location significantly correlated with disability as measured by the EDSS score ($p < 0.01$) (Table 3). No significant differences based on disability and disease duration stratification were seen for the lesions with CVS and paramagnetic rim (Tables 4 and 5).

Discussion

This is the first study to elaborate on the lesion features of Chinese patients with MS based on 7-T MRI,

Figure 1. Sample images from the imaging protocol used in the present study. (A–C), Representative cases of cortical, juxtacortical, periventricular and infratentorial lesion. Row (A) showed lesions on T1-MPRAGE and row (B) showed the same lesion on T2-FLAIR, and row (C) showed the same lesion on FLAWS (magnified views are in the insets). (D and E), Representative cases of central vein sign (CVS) in cortical, juxtacortical, periventricular, and infratentorial lesions. Row (D) showed lesions on T1-MPRAGE and row (E) showed the same lesion with CVS on T2*WI (magnified views are in the insets). (F–H), Representative cases of paramagnetic rim in cortical, juxtacortical, periventricular, and infratentorial lesions. Row (F) showed lesions on T1-MPRAGE and row (G) showed lesions on SWI and row (H) showed the same lesion with paramagnetic rim on SWI-phase image (magnified views are in the insets).

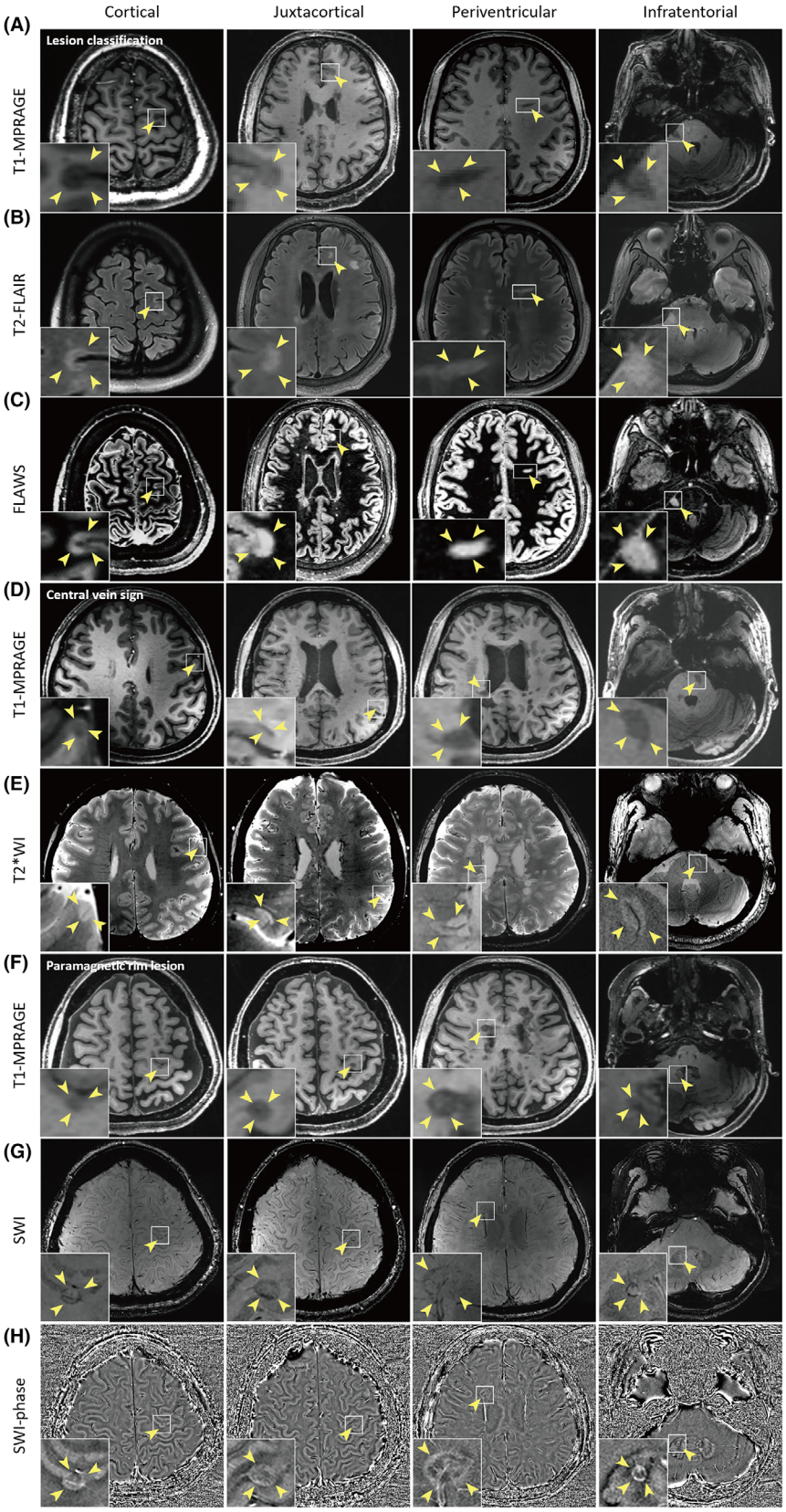

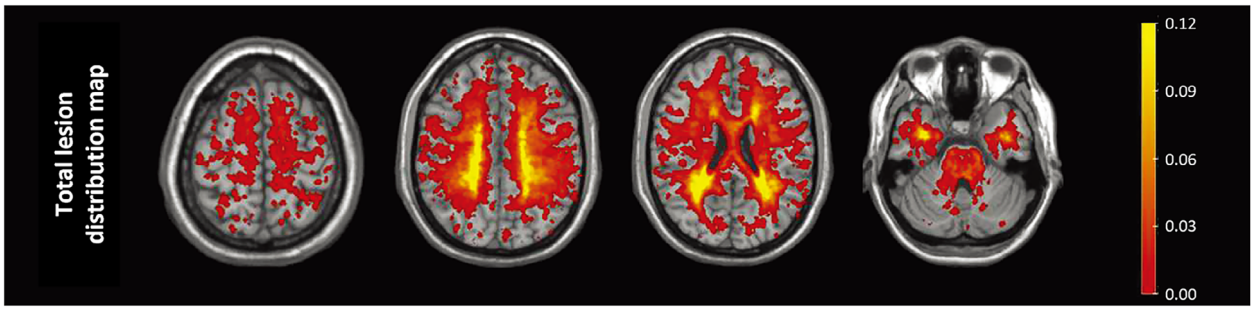

Figure 2. Lesion distribution map for total lesion in Chinese MS patients. The color scale represents the minimum to maximum probability of a lesion occurring in a particular spatial location.

including brain lesion distribution and proportion of CVS and paramagnetic rim. Lesion burden is heavy in Chinese patients with MS. The median lesion count was 45 (IQR, 18–90). Moreover, 21% of lesions and 87% of patients exhibited a paramagnetic rim. The CVS was also common and appeared in 63% lesions from 98% patients.

In this Chinese MS cohort, the proportion of CL (5%) was the least frequent lesion type observed. The sum of juxtacortical (26%) and periventricular (23%) lesions amounted to nearly half of the total lesion count. CLs have emerging value in the diagnostic performance of MS. Cortical inflammation, especially subpial inflammation, is an MS-specific pathology and a potential hallmark of a progressive disease course. 7-T MRI improves CL detection in MS compared to clinical field strengths.[21,22] In a systematic review on imaging of cortical MS lesions at 7T-MRI, the majority of studies (12 out of 17 studies) reported CLs in at least 90% of patients. Across all studies, the mean CL number was 17 $\pm$ 6 per patient.[23] However, only 58% of Chinese patients with MS showed a CL, and the mean CL number was 4 $\pm$ 6 per patient. In our literature review, the 25th percentile of the CL prevalence at patient-level (89%) was still much higher than the prevalence observed in our cohort (58%). Nevertheless, the prevalence in some studies was comparable to the frequency in our cohort. The reason for this difference may be related to the heterogeneity of the studies in the literature review, such as differences in demographic characteristics and MRI parameters. However, as the patients in our cohort were all Chinese, the differences are likely due to ethnicity, genetic, and environment factors. The pathology of CLs is complex and diverse, involving the combined action of T cell, B cell, complement, and so on.[24,25] In other diseases, such as lung cancer, differences in the inflammatory microenvironment of lesions have been confirmed between Chinese and Western population.[26,27] Differences in the extent of CLs may also share similar cause.

In the Chinese MS cohort investigated herein, we found a high frequency of PRLs. In our cohort, 87% (104/120) of the patients had PRLs, with 21% of the lesions exhibiting a paramagnetic rim. Of note, only 49% of patients with PRL were being treated with disease-modifying therapy. PRLs are suggested to reflect the presence of chronic inflammation at the lesion edge, specifically the accumulation of residual and detrimental iron-laden microglia/macrophages after acute inflammation resolution,[13,28] which is considered the hallmark of chronic active lesions. Plenty of signaling pathways, which are involved in iron/heme metabolism, mitotic spindle, hypoxia, and antigen presentation, are highly relevant to MS pathophysiology, especially at the chronic active lesions.[29,30] A high proportion of PRLs may thus indicate an increased risk of disease progression in Chinese patients with MS.[14,31]

Consistent with previously published data, we observed a high frequency of CVS lesions in our MS cohort. 98% of the patients had positive CVS lesions, while 63% of all lesions were exhibiting a CVS. In our cohort, there was no significant difference in the frequency of CVS in patients with different disease duration and EDSS score. Our data support the previously proposed '40% cut-off rule' which is suggested to be specific for MS. This criterion was first proposed by Evangelou et al.[32] According to the '40% rule', a cut-off value of 40% is recommended to radiologically distinguish MS from non-MS disease states. It is suggested that the specificity of the CVS arises as a result of tissue remodeling after disruption of the blood–brain barrier in postcapillary venules at the time of lesion onset. Of note, recent studies have shown that the diagnostic performance of CVS is better than that of CL and PRL.[13,33]

Polygenic inheritance plays a pivotal role in driving MS susceptibility. There are profound and replicable associations between polygenic inheritance and risk assessment of tissue damage and imaging outcomes in cohorts of European descent. These associations might be related to

Table 2. Lesion burden stratified by clinical categories by 7-T MRI.

	Clinical phenotype, median (range) (interquartile ranges)			Disability severity, median (range) (interquartile ranges)		Disease duration, median (range) (interquartile ranges)	
Characteristic	All MS (n = 120)	RRMS (n = 111)	PMS (n = 9)	EDSS Score ≤ 3.0 (n = 97)	EDSS Score > 3.0 (n = 23)	≤3 years (n = 60)	>3 years (n = 60)
Cortical							
Lesion count, n	1 (0–43) (1, 5)	1 (0–43) (0, 4)	2 (0–30) (2, 16)	1 (0–43) (0, 4)	2 (0–30) (1, 12)[b]	1 (0–14) (0, 3)	2 (0–43) (0, 7)
Lesion count, percentage	2.7 (0–38.9) (0, 5.7)	2.3 (0–38.9) (0, 5.3)	3.9 (0–13.0) (2.7, 9.9)	1.8 (0–38.9) (0, 5.1)	3.9 (0–13.0) (1.8, 10.0)[b]	1.8 (0–38.9) (0, 4.4)	3.1 (0–21.8) (0, 7.5)
Lesion volume, mm^3	37 (0–1546) (0, 195)	19 (0–1546) (0, 192)	101 (0–901) (54, 821)[a]	9 (0–811) (0, 144)	101 (0–1545.5) (18, 593)[b]	14 (0–811) (0, 88)	80 (0–1546) (0, 297)[c]
Juxtacortical							
Lesion count	6 (0–184) (2, 20)	5 (0–173) (2, 20)	11 (0–184) (5, 36)	5 (0–173) (2, 14)	16 (0–184) (11, 53)[b]	5 (0–173) (2, 13)	7 (0–184) (2, 24)
Lesion count, percentage	16.2 (0–86.3) (7.8, 25.7)	16.1 (0–86.3) (7.7, 25.9)	21.3 (0–49.7) (11.3, 27.0)	15.8 (0–86.3) (6.5, 24.0)	22.2 (0–49.7) (14.4, 31.2)[b]	16.4 (0–86.3) (8.2, 25.0)	16.3 (0–58.9) (7.7, 28.9)
Lesion volume, mm^3	490 (0–17911) (113, 1384)	447 (0–17911) (104, 1336)	1006 (0–7659) (261, 3641)	353 (0–17911) (97, 1182)	1097 (0–9759) (644, 4243)[b]	347 (0–8744) (76, 990)	892 (0–17911) (214, 2602)[c]
Periventricular							
Lesion count	13 (0–62) (5, 23)	13 (0–62) (5, 23)	18 (1–47) (15, 34)	11 (0–62) (4, 23)	19 (1–51) (12, 33)[b]	11 (0–44) (4, 23)	13 (0–62) (7, 24)
Lesion count, percentage	30.2 (0–84.2) (17.2, 38.7)	30.6 (0–84.2) (16.9, 38.8)	25.0 (12.7–53.2) (20.7, 40.6)	30.6 (0–77.8) (17.3, 39.0)	25.0 (8.1–84.2) (13.8, 35.2)	29.5 (0–84.2) (16.7, 39.7)	31.6 (0–77.8) (17.4, 38.3)
Lesion volume, mm^3	2501 (0–40736) (769, 5231)	2227 (0–40736) (743, 5078)	4005 (132–14265) (1536, 6269)	2008 (0–21227) (628, 4793)	4200 (132–40736) (1656, 8734)[b]	1466 (0–16801) (307, 4140)	3967 (0–40736) (1383, 7345)[c]
Infratentorial							
Lesion count	3 (0–38) (0,7)	3 (0–38) (0, 7)	3 (0–21) (2, 14)	2 (0–38) (0, 6)	5 (0–31) (3, 19)[b]	3 (0–38) (0, 6)	3 (0–31) (0, 8)
Lesion count, percentage	5.8 (0–100.0) (0.4, 11.9)	5.7 (0–100.0) (0, 12.2)	8.1 (0–25.0) (3.4, 9.5)	5.2 (0–100.0) (0, 12.5)	8.1 (0–26.3) (5.4, 9.6)	6.7 (0–80.0) (0.4, 16.7)	5.2 (0–100.0) (0.7, 9.1)
Lesion volume, mm^3	144 (0–3247) (1, 500)	165 (0–3247) (0, 507)	125 (0–2096) (68, 734)	115 (0–2801) (0, 384)	311 (0–3247) (142, 1591)[b]	154 (0–2801) (5, 533)	144 (0–3247) (1, 500)
Total							
Lesion count	45 (2–370) (18, 90)	39 (2–356) (17, 90)	54 (4–370) (42, 152)	31 (0–343) (16, 85)	73 (4–370) (51, 180)[b]	37 (4–343) (13, 77)	52 (2–370) (21, 115)
Lesion volume, mm^3	5240 (18–62599) (2326, 11686)	4809 (18–62599) (1865, 11697)	6904 (229–31502) (5173, 11817)	4222.68 (18–42199) (1287, 9106)	7327 (229–62599) (5832, 15549)[b]	3624 (70–32819) (920, 8307)	6840 (18–62599) (3178, 14501)[c]

[a]$p < 0.05$ for difference from RRMS.

[b]$p < 01.05$ for difference from EDSS Score ≤ 3.0.

[c]$p < 0.05$ for difference from disease duration ≤ 3 years.

Table 3. Correlation of magnetic resonance imaging indices with EDSS.

	Cortical		Juxtacortical		Periventricular		Infratentorial		Total	
Characteristic	Count	Volume	Count	Volume	Count	Volume	Count	Volume	Count	Volume
EDSS	0.30*	0.31*	0.27*	0.22*	0.28*	0.31*	0.30*	0.32*	0.31*	0.35*

*p <0.01.

Table 4. Lesions with central vein sign stratified by clinical categories by 7-T MRI.

	Clinical phenotype, median (range)			Disability severity, median (range)		Disease duration, median (range)	
Characteristic	All MS (n = 120)	RRMS (n = 111)	PMS (n = 9)	EDSS Score ≤3.0 (n = 97)	EDSS Score > 3.0 (n = 23)	≤3 years (n = 60)	>3 years (n = 60)
Cortical							
Positive CVS lesion count	0 (0–14)	0 (0–12)	2 (0–14)	0 (0–10)	1 (0–14)	0 (0–12)	0.5 (0–14)
Positive CVS lesion percentage	50% (0%–100%)	50% (0%–100%)	57% (0%–100%)	50% (0%–100%)	33% (0%–100%)	50% (0%–100%)	48% (0%–100%)
Juxtacortical							
Positive CVS lesion count	3.5 (0–93)	3 (0–93)	8 (0–84)	3 (0–93)	9 (0–84)	3 (0–93)	4.5 (0–84)
Positive CVS lesion percentage	60% (0%–100%)	57% (0%–100%)	81% (44%–100%)	60% (0%–100%)	55% (27%–100%)	54% (0%–100%)	64% (0%–100%)
Periventricular							
Positive CVS lesion count	7 (0–49)	6 (0–49)	11 (1–33)	6 (0–49)	11 (0–33)	5 (0–27)	8 (0–49)
Positive CVS lesion percentage	60% (0%–100%)	59% (0%–100%)	69% (33%–100%)	61% (0%–100%)	57% (0%–100%)	59% (0%–100%)	63% (0%–100%)
Infratentorial							
Positive CVS lesion count	2 (0–29)	2 (0–29)	3 (0–19)	1 (0–29)	4 (0–20)	1 (0–29)	2 (0–20)
Positive CVS lesion percentage	75% (0%–100%)	74% (0%–100%)	95% (57%–100%)	76% (0%–100%)	74% (0%–100%)	68% (0%–100%)	80% (0%–100%)
Total							
Positive CVS lesion count	25.5 (0–232)	24 (0–232)	41 (4–210)	20 (0–232)	46 (1–210)	22 (0–232)	31 (2–210)
Positive CVS lesion percentage	71% (0%–100%)	71% (0%–100%)	74% (57%–100%)	71% (0%–100%)	68% (5%–100%)	70% (0%–94%)	71% (5%–100%)

There is no significant difference between groups.
CVS, central vein sign.

Table 5. Lesions with paramagnetic rim stratified by clinical categories by 7-T MRI.

Characteristic	Clinical phenotype, median (range)			Disability severity, median (range)		Disease duration, median (range)	
	All MS (n = 120)	RRMS (n = 111)	PMS (n = 9)	EDSS Score ≤3.0 (n = 97)	EDSS Score > 3.0 (n = 23)	≤3 years (n = 60)	>3 years (n = 60)
Cortical							
PRL count	0 (0–5)	0 (0–4)	0 (0–5)	0 (0–4)	0 (0–5)	0 (0–4)	0 (0–5)
PRL percentage	0% (0%–100%)	3% (0%–100%)	0% (0%–20%)	0% (0%–100%)	0% (0%–33%)	0% (0%–100%)	3% (0%–50%)
Juxtacortical							
PRL count	1 (0–53)	1 (0–53)	0 (0–32)	1 (0–53)	2 (0–39)	1 (0–53)	1 (0–39)
PRL percentage	9% (0%–100%)	9% (0%–100%)	3% (0%–27%)	9% (0%–100%)	8% (0%–38%)	14% (0%–83%)	7% (0%–100%)
Periventricular							
PRL count	2 (0–27)	2 (0–27)	2 (0–16)	2 (0–27)	3 (0–16)	1 (0–14)	2 (0–27)
PRL percentage	17% (0%–100%)	16% (0%–100%)	18% (0%–100%)	15% (0%–100%)	20% (0%–100%)	15% (0%–100%)	17% (0%–100%)
Infratentorial							
PRL count	0 (0–9)	0 (0–9)	0 (0–3)	0 (0–9)	0 (0–3)	0 (0–9)	0 (0–3)
PRL percentage	0% (0%--100%)	0% (0%–100%)	0% (0%–67%)	0% (0%–100%)	0% (0%–67%)	0% (0%–50%)	0% (0%–100%)
Total							
PRL count	6 (0–101)	6 (0–101)	5 (1–84)	5 (0–101)	14 (0–84)	6 (0–101)	6 (0–92)
PRL percentage	16% (0%–67%)	16% (0%–67%)	23% (0%–27%)	17% (0%–67%)	16% (0%–30%)	20% (0%–67%)	15% (0%–44%)

There is no significant difference between groups.
PRL, paramagnetic rim lesion.

the fact that polygenic inheritance is involved in mediating the inflammatory signaling, response to viral infection, oxidative damage, RNA polymerase transcription, and epigenetic regulation of gene expression. In these cohorts of European descent, significant association of genetic predisposition with thalamic atrophy was observed.[2] Given the significant relationship between genetic features and inflammatory mechanisms, the study of genetic inheritance might also increase the understanding of the lesion characteristics in Chinese patients in future investigations.

There are some limitations to our study. We did not combine the genomic information from Chinese people for our analysis, hence the weight of genes affecting the differences in MS lesions observed is unknown. Furthermore, the lack of a longitudinal follow-up also affects the reliability of our study findings. In addition, the number of patients with progressive MS that were examined in our study is relatively small. Therefore, our conclusions need to be validated in the future by combining genetic information and increased cohort size.

In conclusion, our study elaborated on lesion morphology of Chinese patients with MS at 7-T MRI. We found that lesion burden is heavy in Chinese patients with MS. Moreover, the proportion lesions exhibiting CVS and paramagnetic rims is relatively high and comparable to the numbers observed at 7-T MRI in MS patients from other ethnic groups. Hence, the management and research of Chinese patients with MS needs to be further strengthened. Future research should combine clinical and MR features together with the genomic information from Chinese people to further understand the pathophysiology of 7-T MRI characteristics and their clinical significance in Chinese patients with MS.

Author Contributions

F.-D.S. formulated the study concept; L.S. and Z.Z. designed the study and drafted the manuscript. F.-D.S., P.H., Y.D., F.P., and Y.L. completed data interpretation. Z.Z. optimized the MR scan parameters. C.G., A.G., M.Z., X.S., X.L., T.S., W.X., H.W., J.J., and D.-C.T. performed the experiments and data collection. L.S., Z.Z., and J.K. prepared the figures and analyzed the data.

Acknowledgments

This study was supported partly by National Science Foundation of China Grant 81830038, 82271329. We recognize colleagues from the Tiantan Neuroimaging Center of Excellence (T-NICE) for their assorted support. We want to thank Zhu Wanlin for his excellent technical support.

Conflict of Interest

The authors have no conflicts of interest to declare.

Data Availability Statement

The de-identified data will be available for investigators following approval from the Institutional Review Board of China National Clinical Research Center for Neurological Diseases (Beijing, China).

References

1. Thompson AJ, Banwell BL, Barkhof F, et al. Diagnosis of multiple sclerosis: 2017 revisions of the McDonald criteria. Lancet Neurol. 2018;17(2):162-173.
2. Shams H, Shao X, Santaniello A, et al. Polygenic risk score association with multiple sclerosis susceptibility and phenotype in Europeans. Brain. 2023;146(2):645-656.
3. Kister I, Chamot E, Bacon JH, et al. Rapid disease course in African Americans with multiple sclerosis. Neurology. 2010;75(3):217-223.
4. Caldito NG, Saidha S, Sotirchos ES, et al. Brain and retinal atrophy in African-Americans versus Caucasian-Americans with multiple sclerosis: a longitudinal study. Brain. 2018;141(11):3115-3129.
5. Tian DC, Zhang C, Yuan M, et al. Incidence of multiple sclerosis in China: a nationwide hospital-based study. Lancet Reg Health West Pac. 2020;1:100010.
6. Jia D, Zhang Y, Yang C. The incidence and prevalence, diagnosis, and treatment of multiple sclerosis in China: a narrative review. Neurol Sci. 2022;43(8):4695-4700.
7. Ochi H, Fujihara K. Demyelinating diseases in Asia. Curr Opin Neurol. 2016;29(3):222-228.
8. Qiu W, James I, Carroll WM, Mastaglia FL, Kermode AG. HLA-DR allele polymorphism and multiple sclerosis in Chinese populations: a meta-analysis. Mult Scler. 2011;17 (4):382-388.
9. Qiu W, Huang DH, Hou SF, et al. Efficacy and safety of Teriflunomide in Chinese patients with relapsing forms of multiple sclerosis: a subgroup analysis of the phase 3 TOWER study. Chin Med J. 2018;131(23):2776-2784.
10. Harrison DM, Roy S, Oh J, et al. Association of Cortical Lesion Burden on 7-T magnetic resonance imaging with cognition and disability in multiple sclerosis. JAMA Neurol. 2015;72(9):1004-1012.
11. Sinnecker T, Clarke MA, Meier D, et al. Evaluation of the central vein sign as a diagnostic imaging biomarker in multiple sclerosis. JAMA Neurol. 2019;76 (12):1446-1456.
12. Chaaban L, Safwan N, Moussa H, El-Sammak S, Khoury SJ, Hannoun S. Central vein sign: a putative diagnostic marker for multiple sclerosis. Acta Neurol Scand. 2022;145 (3):279-287.
13. Maggi P, Sati P, Nair G, et al. Paramagnetic rim lesions are specific to multiple sclerosis: an international multicenter 3T MRI study. Ann Neurol. 2020;88 (5):1034-1042.
14. Borrelli S, Martire MS, Stölting A, et al. Central vein sign, cortical lesions, and paramagnetic rim lesions for the diagnostic and prognostic workup of multiple sclerosis. Neurol Neuroimmunol Neuroinflamm. 2024;11(4):e200253.
15. Clarke WT, Mougin O, Driver ID, et al. Multi-site harmonization of 7 tesla MRI neuroimaging protocols. NeuroImage. 2020;206:116335.
16. Haller S, Haacke EM, Thurnher MM, Barkhof F. Susceptibility-weighted imaging: technical essentials and clinical neurologic applications. Radiology. 2021;299(1):3-26.
17. Sinnecker T, Schumacher S, Mueller K, et al. MRI phase changes in multiple sclerosis vs neuromyelitis optica lesions at 7T. Neurol Neuroimmunol Neuroinflamm. 2016;3(4):e259.
18. Sati P, Oh J, Constable RT, et al. The central vein sign and its clinical evaluation for the diagnosis of multiple sclerosis: a consensus statement from the north American imaging in multiple sclerosis cooperative. Nat Rev Neurol. 2016;12(12):714-722.
19. Absinta M, Sati P, Masuzzo F, et al. Association of Chronic Active Multiple Sclerosis Lesions with Disability in Vivo. JAMA Neurol. 2019;76(12):1474-1483.
20. Yan Y, Li Y, Fu Y, et al. Autoantibody to MOG suggests two distinct clinical subtypes of NMOSD. Sci China Life Sci. 2016;59(12):1270-1281.
21. de Graaf WL, Kilsdonk ID, Lopez-Soriano A, et al. Clinical application of multi-contrast 7-T MR imaging in multiple sclerosis: increased lesion detection compared to 3 T confined to grey matter. Eur Radiol. 2013;23(2):528-540.
22. Sinnecker T, Mittelstaedt P, Dörr J, et al. Multiple sclerosis lesions and irreversible brain tissue damage: a comparative ultrahigh-field strength magnetic resonance imaging study. Arch Neurol. 2012;69(6):739-745.
23. Madsen MAJ, Wiggermann V, Bramow S, Christensen JR, Sellebjerg F, Siebner HR. Imaging cortical multiple sclerosis lesions with ultra-high field MRI. NeuroImage Clinical. 2021;32:102847.
24. Bhargava P, Hartung HP, Calabresi PA. Contribution of B cells to cortical damage in multiple sclerosis. Brain. 2022;145(10):3363-3373.
25. Calabrese M, Filippi M, Gallo P. Cortical lesions in multiple sclerosis. Nat Rev Neurol. 2010;6(8):438-444.
26. Wang C, Yin R, Dai J, et al. Whole-genome sequencing reveals genomic signatures associated with the inflammatory microenvironments in Chinese NSCLC patients. Nat Commun. 2018;9(1):2054.
27. Zhang XC, Wang J, Shao GG, et al. Comprehensive genomic and immunological characterization of Chinese non-small cell lung cancer patients. Nat Commun. 2019;10 (1):1772.

28. Calvi A, Clarke MA, Prados F, et al. Relationship between paramagnetic rim lesions and slowly expanding lesions in multiple sclerosis. Mult Scler. 2023;29 (3):352-362.
29. Maggi P, Bulcke CV, Pedrini E, et al. B cell depletion therapy does not resolve chronic active multiple sclerosis lesions. EBioMedicine. 2023;94:104701.
30. Absinta M, Maric D, Gharagozloo M, et al. A lymphocyte-microglia-astrocyte axis in chronic active multiple sclerosis. Nature. 2021;597(7878):709-714.
31. Cagol A, Benkert P, Melie-Garcia L, et al. Association of Spinal Cord Atrophy and Brain Paramagnetic rim Lesions with Progression Independent of relapse activity in people with MS. Neurology. 2024;102(1):e207768.
32. Tallantyre EC, Dixon JE, Donaldson I, et al. Ultra-high-field imaging distinguishes MS lesions from asymptomatic white matter lesions. Neurology. 2011;76(6):534-539.
33. Cagol A, Cortese R, Barakovic M, et al. Diagnostic performance of cortical lesions and the central vein sign in multiple sclerosis. JAMA Neurol. 2024;81(2):143-153.

Supporting Information

Additional supporting information may be found online in the Supporting Information section at the end of the article.

Data S1:

